International Research Journal of Engineering and Technology (IRJET) e-ISSN: 2395-0056
Volume: 11 Issue: 07 | July 2024 www.irjet.net p-ISSN: 2395-0072

Comparative Analysis of Regulated Metal Deposition (RMD) and Flux-Cored Arc Welding (FCAW) on 316LN Stainless Steel: Effects of Welding Parameters on Weld Bead Characteristics

Ravi Dave[1,2], Indravadan B. Dave[3*], Jay J. Vora[4*], Subhash Das[5], Sonam Patel[2]

[1]Research Scholar, Gujarat Technological University, Ahmedabad, India
[2]Metallurgy Engineering Department, Dr. S. and S. S. Ghandhy College of Engineering and Technology, Surat, India.
[3]Metallurgy Engineering Department, Government Engineering College, Sector 28, Gandhinagar, India
[4]Mechanical Engineering Department, Pandit Deendayal Energy University, Gandhinagar, India,
[5]ITW India Private Limited, Vadodara, India

Abstract:

This study aims to systematically investigate and compare the effects of key welding parameters on weld bead characteristics in regulated metal deposition (RMD) and flux-cored arc welding (FCAW) processes when applied to bead-on-plate welding on 316LN stainless steel. This research focuses on understanding the relationships between welding parameters such as current, voltage, and heat input and weld bead dimensions such as bead width, height, depth of penetration, and width of the heat-affected zone for both techniques. The overall quality of the welds produced by each technique is examined through visual inspection, liquid penetrant testing, and macroscopic and microscopic examinations. Through this comparative analysis of the RMD and FCAW processes, this research aims to provide valuable insights into the selection of welding parameters for 316LN stainless steel, thereby improving weld quality and efficiency in industrial applications. The results indicate that in both RMD and FCAW, a higher current increases bead dimensions and penetration, whereas a higher voltage produces wider beads but reduces height and penetration. In FCAW, the higher heat input produces a wider HAZ than RMD does.

Keywords: regulated metal deposition (RMD) technique, flux cored arc welding (FCAW), 316LN, bead-on plate trials, governing variables, weld bead dimensions

1. Introduction:

Stainless steels enriched with nitrogen possess a special combination of properties that make them ideal in various industries where strength, corrosion resistance, and high-temperature mechanical performance are crucial. The use of these materials as cost-effective alternatives to other materials further enhances their value in engineering and manufacturing applications [1, 2]. 316LN is a variant of low-carbon austenitic stainless steel that plays an important role as an essential structural component in various sectors, including chemical processing, transportation, storage, and nuclear industries, owing to its advantageous high-temperature mechanical properties, compatibility with liquid sodium, good weldability, good irradiation resistance, and adequate experience in the use of these materials in sodium-cooled reactors [3–5]. The 316LN material demonstrates favorable plasticity and relatively high impact toughness, particularly under cryogenic conditions. In the context of joining these structural materials, arc welding is the preferred technique because of its compatibility with their properties [6, 7].

SMAW and TIG welding are commonly used for the initial root pass in a weld joint. However, these methods have certain limitations, including time-consuming procedures and inconsistent weld characteristics [8, 9]. On the other hand, GMAW, which is suitable for filling, faces challenges in the root pass because of issues such as spatter formation [10]. In this context, the introduction of a modified short-circuiting process represents an exciting opportunity to increase the efficiency and effectiveness of root-pass welding [11, 12].

Regulated Metal Deposition (RMD), introduced by Miller Electric in 2004, is an advanced short-circuiting arc welding process that involves managing welding during each short-circuit phase and adjusting the waveform on the basis of material properties [13, 14]. Precisely regulated metal transfer ensures the consistent deposition of droplets, greatly simplifying the

welder's ability to manage the molten puddle [15]. A thorough grasp of the controlled short-circuit mechanism is gained by segmenting a standard RMD cycle into seven distinct phases, as outlined by Das et al. [16]. Compared with TIG and MIG welding, this process offers significant advantages, such as a faster welding speed (6–12 inches per minute), resulting in three times faster production and reduced rework. The RMD process allows for a root pass depth of 3.2 to 6.4 mm, eliminating the need for hot passes and increasing the welding efficiency [17]. It also minimizes heat input, reducing material distortion and the risk of issues such as cold laps and spatter. These benefits lead to superior weld quality and increased productivity [18, 19]. Din Bandhu et al. compared RMD and GMAW on ASTM A387-11-2 steel plates. They reported that RMD produced deeper penetration, a smaller heat-affected zone, and lower hardness across all weldment zones than did GMAW [20]. Din Bandhu et al. studied the effects of metal-cored filler wire on RMD-welded low-alloy steel plates. The as-welded plates presented typical dendritic surfaces, whereas the heat-treated plates presented finer, irregular martensitic structures in the weld zone [21].

Flux-Cored Arc Welding (FCAW) uses flux-filled tubular wire to shield the weld pool and prevent contamination. This is unique because it contains flux within the continuous wire electrode, which improves the number of operator duty cycles [22]. Compared with shielded metal arc welding (SMAW), FCAW provides higher deposition efficiency and faster deposition rates for austenitic stainless steels, and it offers better penetration. This process is widely adopted by industries to increase welding productivity. Recently, there has been a notable increase in the utilization of FCAW because of its numerous advantages. These include its efficiency in effectively depositing weld metal, compatibility with automation, adaptability to various welding positions, user-friendliness relative to alternative methods, capacity to produce high-quality welding seams, and cost-effectiveness when joining thick materials [23]. A study by Ronaldo R. De Paz investigated how 43 companies worldwide use FCAW. Research has shown that FCAW is still widely used because it is easy to work with. Companies rated FCAW products highly for quality and performance, both domestically (4.6) and abroad (4.33) [24]. Amit Kumar compared FCAW and MIG welding for repairing damaged low-Cr-Mo alloy steel boiler tubes. FCAW-welded samples presented higher tensile and yield strengths than MIG-welded samples did [25]. Several studies have examined the effects of welding parameters on bead geometry in various welding processes. Shoeb et al. [26] and I.S. Kim et al. [27] reported that higher currents increased the penetration depth and bead width in the MIG and GMAW processes, respectively. Both studies noted that higher voltages resulted in wider beads. P.K. Palani et al. [28] observed an increased penetration area with increasing current when flux-cored wire was used on structural steel. Similarly, Memduh Kurtulmus et al. [29] reported that a higher current increased the reinforcement height and penetration depth in flux-cored arc welding, whereas a higher voltage widened the bead. Deb Kumar Adak et al. [30] found that a greater heat input increased the HAZ width in the GMAW of mild steel. These findings consistently demonstrate the significant influence of the welding parameters on the bead geometry and weld characteristics across different materials and welding techniques.

The literature available in the public domain extensively covers welding techniques such as submerged arc welding (SAW), gas tungsten arc welding (GTAW), and gas metal arc welding (GMAW) and examines welding performance parameters such as the heat-affected zone, penetration depth, and weld bead geometry [31–35]. However, there is a noticeable research gap in the context of advanced GMAW processes, particularly those related to modified short-circuit metal transfer, as seen in the RMD technique. This unexplored area holds promise for further investigation. With limited research papers available on the RMD technique, it is noteworthy that this method remains largely unexplored for welding stainless steels of grade 316LN, as observed from literature surveys. Therefore, its application in this context represents a novelty. Additionally, the FCAW process is gaining widespread acceptance among industries; there has been no previous comparison between the FCAW and RMD processes. This comparison is anticipated to produce intriguing results and simplify process selection. In the present study, bead-on-plate trials were conducted on 316LN base metal via two distinct methods: the Regulated Metal Deposition (RMD) technique with 316 L solid wire and the Flux Cored Arc Welding (FCAW) technique with 316 L flux-cored wire. The objective of this research is to aesthetically evaluate and compare bead-on-plate welding deposited by two distinct welding processes: RMD and FCAW. This work aims to assess the influence of variables such as current, voltage, and heat input rates on various welding performance characteristics, such as the heat-affected zone, depth of penetration, bead width, and bead height.

2. Experimental work:

2.1. Base material and filler wire

In this work, austenitic stainless steel (316LN) was selected as the base metal. Two different filler wires were used for the experiments, namely, AWS A5.9: ER316L solid wire for the RMD technique and AWS A5.22: E316LT1-4 flux-cored wire for the FCAW technique. Both filler wires have a diameter of 1.2 mm. The chemical compositions and mechanical properties of these filler wires and the base metal are outlined in Tables 1 and 2, respectively. The initial plate, with a thickness of 40 mm, was precision machined into samples measuring 8 mm × 200 mm × 750 mm via a wire-cut EDM machine. Separate samples were prepared for both the RMD and FCAW trials.

Table 1 – Chemical composition of the filler wire and base metal[a].

Content (%wt.)	Base Metal SA240 Gr. 316LN	Solid Wire ER316L	Flux Cored Wire E316LT1-4
Carbon	0.026	0.012	0.030
Manganese	1.85	1.59	1.26
Silicon	0.59	0.39	0.51
Sulphur	0.013	0.013	0.01
Phosphorous	0.030	0.021	0.03
Chromium	17.65	18.33	18.63
Nickel	12.23	12.17	12.14
Molybdenum	2.89	2.53	2.88
Nitrogen	0.11	0.037	--
Other Element	--	--	Cu = 0.04

[a] Taken from actual test certificates.

Table 2 – Mechanical properties of the filler wire and base metal[a].

Mechanical property	Base Metal	Solid Wire	Flux Cored Wire
Tensile strength (MPa)	549	590	641
Yield strength (MPa)	258	--	--
Elongation	50.2%	39%	36%

[a] Taken from actual test certificates.

2.2. Welding Trials

A Miller Pipe Worx 400 machine was employed for both the RMD and FCAW processes. This machine is a multiprocess machine that includes conventional stick, DC TIG, flux-cored, and MIG welding processes. It also features advanced RMD and pulsed MIG processes. The machine is shown in Figure 1.

Figure 1 Miller make: Pipe Worx 400 welding power source

Following ASME Section IX, a certified welder performed manual welding in the 1G position. For a high-quality weld, the selection of welding parameters—such as current, voltage, and gas flow rate is essential. These parameters were chosen after consulting industry experts and consumable suppliers, as well as reviewing the relevant literature. To confirm the welding settings on the basis of weld bead profiles, bead-on-plate testing was carried out, combining established approaches with adaptive adjustments for accuracy [31–35]. A total of eighteen bead-on-plate trials were carried out using FCAW and RMD techniques. While the RMD trials employed a gas mixture of 98% argon (Ar) and 2% oxygen (O2), the FCAW studies utilized 80% argon (Ar) and 20% carbon dioxide (CO2). The experiments were conducted on 750 × 200 × 8 mm plates. The plate setup and bead-on-plate welding procedure are shown in Figures 3 and 4, respectively. Tables 2 and 3 provide specific welding parameters for the RMD and FCAW.

Figure 2 Plate setup for bead-on-plate welding.

Figure 3 Original photograph of bead-on-plate welding

Table 3 – Welding Parameter for RMD technique.

Experiment	Current (A)	Voltage (V)	Gas Flow Rate (L/min)
A	80	12	10
B	80	15	15
C	80	18	20
D	110	12	10
E	110	15	15
F	110	18	20
G	140	12	10
H	140	15	15
I	140	18	20

Table 4 – Welding Parameters for FCAW technique.

Experiment	Current (A)	Voltage (V)	Gas Flow Rate (L/min)
1	140	20	10
2	140	22	15
3	140	24	20
4	180	20	10
5	180	22	15
6	180	24	20
7	220	20	10
8	220	22	15
9	220	24	20

The bead-on-plate trials deposited by the RMD technique and FCAW technique are represented in Figures 4 and 5.

Figure 4 Bead-on-plate trials deposited by RMD technique

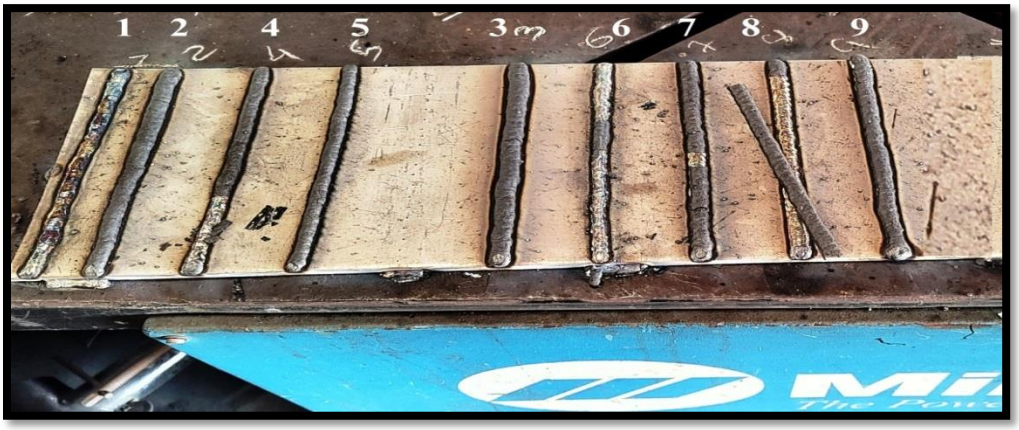

Figure 5 Bead-on-plate trials deposited by FCAW technique

2.3. Visual inspection:

Visual inspection is widely regarded as the most prevalent and cost-effective approach for assessing weld quality. This method involves using the unaided human eye to detect any surface irregularities present within the weld area. This approach offers immediate detection of welding flaws, thereby reducing subsequent repair expenses resulting from detected

imperfections in the weld region. For bead-on-plate welding, this method was used for identifying surface defects such as spatter, porosity, undercut, etc. [20]. Initially, visual inspection was carried out on both the RMD and FCAW bead-on-plate welded samples following a meticulous cleaning process using a stainless steel wire brush.

2.4. Liquid Penetrant Testing (LPT):

The liquid penetrant inspection technique is a reliable approach for identifying discontinuities present on the surfaces of impermeable metals and other similar materials. Common types of flaws that can be successfully detected via this approach include cracks, seams, laps, cold shuts, laminations, and porosity. Liquid penetrant testing was conducted on all the bead-on-plate trials.

2.5. Macroscopic analysis

To investigate the macrostructural characteristics of the bead-on plate welds, bead-on welded plates were sectioned transversely from the central portion of the weld length using a band-saw machine. All the samples underwent a routine polishing process involving the use of SiC abrasives, followed by disc polishing to achieve a mirror-finished surface. For etching, a solution of aqua regia (comprising 15 ml of HCl and 5 ml of HNO3) was used. The etched samples were subsequently examined under a macroscope to measure the required responses, such as depth of penetration (DOP), bead width (BW), and bead height (BH), as shown in Figures 12 and 13. The heat-affected zone (HAZ) was not discernible through a macroscope. Consequently, to measure the width of the HAZ precisely, a microscopic analysis was performed. A prepared mirror-polished sample underwent an etching process and was subsequently subjected to examination using a metallurgical microscope, as shown in Figure 14.

2.6. Heat input calculation

The heat input represents the energy transferred to the weld during welding and is typically measured as the energy per unit length of the weld (e.g., kJ/in or kJ/mm). Below is the formula used to calculate the heat input [36].

$$\mathbf{Q} = \frac{\mathbf{V} \times \mathbf{I}}{\mathbf{S}} \qquad (1)$$

where:

Q = Heat input (kJ/in or kJ/mm), V = Voltage (volts)

I = Current (amps), S = Travel speed (inches per minute or millimeters per minute)

The heat input in welding processes is consistently of great interest, given its influence on the morphology of the weld bead, fusion zone, and microstructures in the heat-affected zone (HAZ), as well as the mechanical behavior of the welded joint [37]. Cortéz et al. [38], in their examination of the impact of heat input on the microstructure and mechanical properties of welded joints, employed the welding energy equation. This equation, derived as the product of the mean current and mean voltage divided by the travel speed, is referred to as heat input. The calculated heat inputs for both the RMD and FCAW processes are shown in Tables 7 and 8.

3. Results and discussion:

3.1. Visual inspection:

During the visual examination of RMD bead-on-plate samples, the examination of Sample A, depicted in Figure 6, revealed a weld bead characterized by a slender width and an uneven shape.

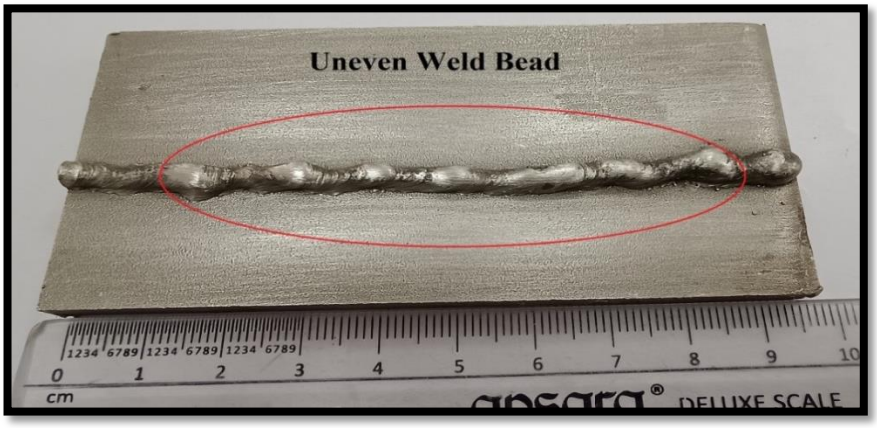

Figure 6 Visual inspection of sample A revealing narrow beads and uneven shapes

Figure 7 Visual inspection of Sample D, which is free from surface defects

Figure 8 Visual inspection of Sample 10 revealing spatters

Figure 9 Visual inspection of Sample 3, which is free from surface defects

This result can be traced back to the application of low current and voltage settings, specifically an 80-ampere current and a 12-volt voltage. On the other hand, visual inspection of the remaining samples confirmed the visual clarity of the weld and the absence of any discernible defects, such as surface porosity and underfill. Moreover, the deposition of filler metal displayed a flawless and uniform distribution throughout the entire length of the weld bead. For visual reference, see Figure 7, illustrating the visual inspection of Sample D, which demonstrates freedom from surface defects.

In the visual examination of the FCAW bead-on-plate samples, the analysis of Sample 10, illustrated in Figure 8, revealed the presence of spatter. This occurrence is attributed to the application of a high welding current of 220 amperes. However, visual examination of the remaining samples confirmed the visual clarity of the welds in the absence of any discernible defects. For visual reference, see Figure 9, which depicts the visual inspection of Sample 3 and shows freedom from surface defects.

3.2. Liquid Penetrant Testing:

The liquid penetrant testing of RMD bead-on-plate welded Sample H, as shown in Figure 10, reveals an undercut in Sample H, as further indicated in Figure 11. This phenomenon may be attributed to the application of a higher welding current. However, during liquid penetrant testing of the remaining RMD and FCAW samples, the exceptional quality of the welds was confirmed. Importantly, inspection revealed the absence of any surface defects.

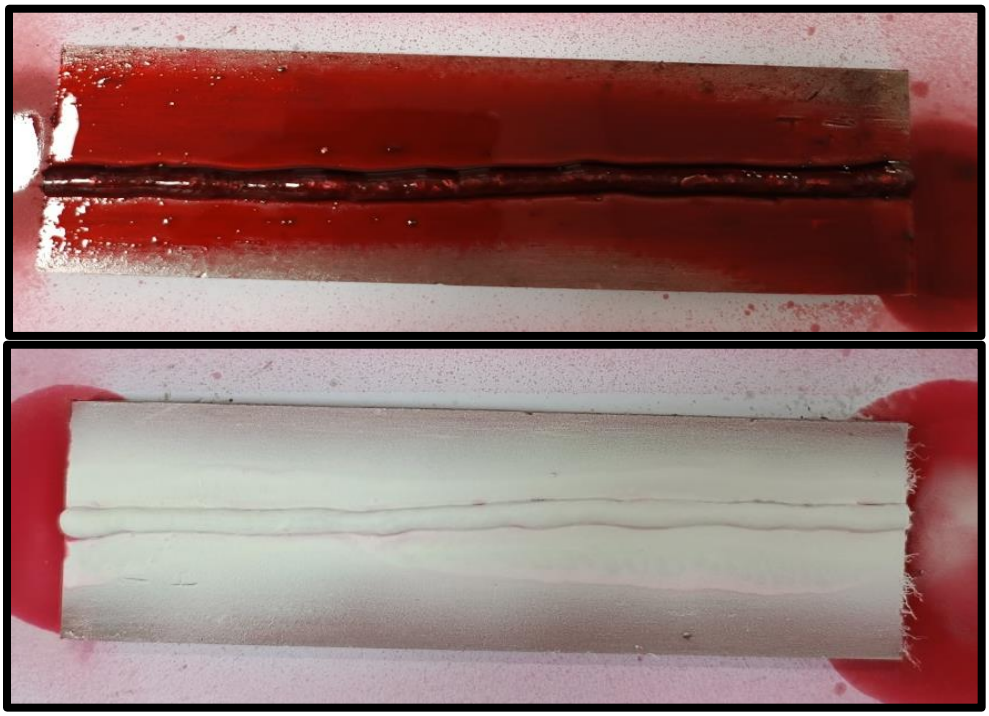

Figure 10 Liquid penetrant testing of sample H

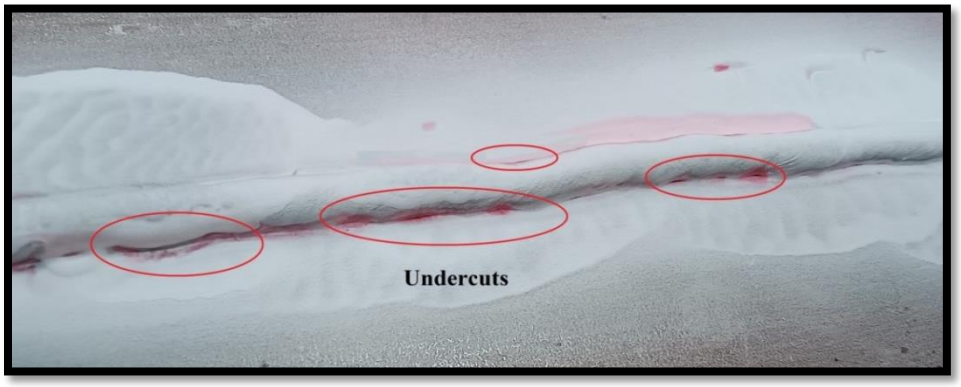

Figure 11 Liquid Penetrant Testing Results Revealing Undercuts in Sample H"

3.3. Macroscopic analysis

The dimensions derived from the macroscopic observations are presented in Tables 7 and 8. The macroscopic images capturing the bead-on-plate welds for both the RMD and FCAW processes are illustrated in Figures 12 and 13, respectively.

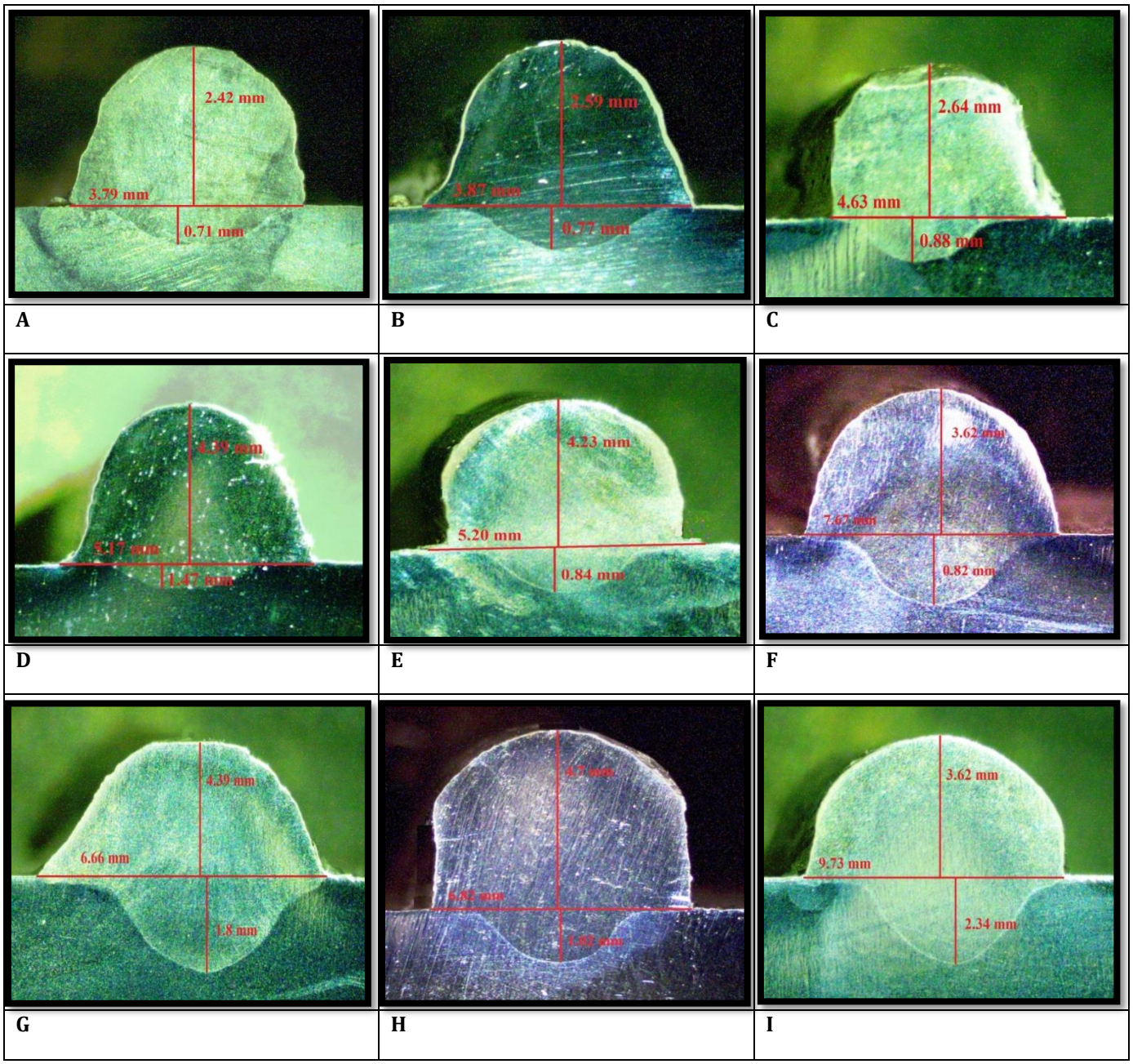

Figure 13 Macroscopic image of an RMD bead on a plate sample

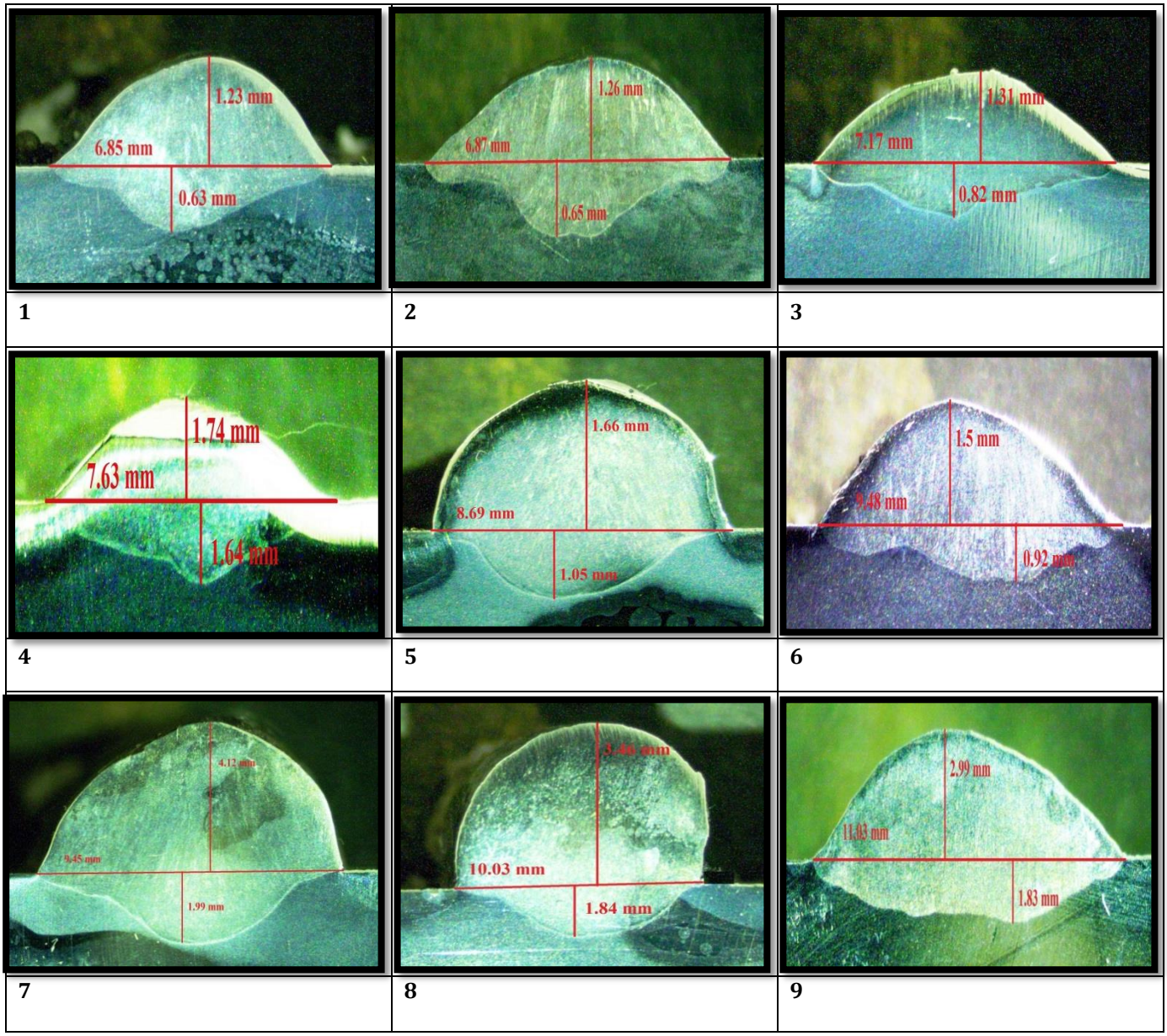

Figure 13 Macroscopic image of an FCAW bead on a plate sample

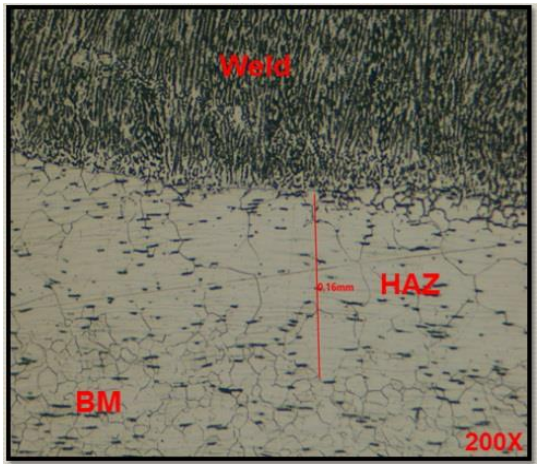

Figure 14 Microscopic analysis for the measurement of the width of the HAZ

Microscopic analysis was conducted to measure the width of HAZ for both RMD and FCAW bead-on-plate samples. The weld bead geometry details for the RMD and FCAW bead-on-plate samples are documented in Tables 5 and 6, respectively.

Table 5 – Detail of Weld bead geometry for RMD bead on plate samples

Sample ID	Bead Width (mm)	Bead Height (mm)	Depth of Penetration (mm)	Width of HAZ (mm)
A	3.79	2.42	0.71	0.1
B	3.87	2.59	0.77	0.14
C	4.63	2.64	0.88	0.19
D	5.17	4.39	1.47	0.21
E	5.20	4.23	0.84	0.2
F	7.67	3.62	0.82	0.21
G	6.66	4.39	1.8	0.23
H	6.82	4.7	1.02	0.28
I	9.73	3.62	2.34	0.26

Table 6 – Detail of Weld bead geometry for FCAW bead on plate samples

Sample ID	Bead Width (mm)	Bead Height (mm)	Depth of Penetration (mm)	Width of HAZ (mm)
1	6.85	1.23	0.63	0.19
2	6.87	1.26	0.65	0.23
3	7.17	1.31	0.82	0.36

4	7.63	1.74	1.64	0.36
5	8.69	1.66	1.05	0.39
6	9.48	1.5	0.92	0.39
7	9.45	4.12	1.99	0.41
8	10.03	3.46	1.84	0.43
9	11.03	2.99	1.83	0.49

3.4. Effect of the welding current:

The impact of the welding current on the bead width, depth of penetration, and bead height at a voltage of 15 volts in the RMD welding technique is presented in Figure 15. Figure 16 shows the corresponding effects of the FCAW welding technique at a voltage of 22 volts. As shown in Figure 16, for the RMD technique, an increase in the welding current correlates with an increase in the weld bead height, width, and depth of penetration. Similarly, as indicated in Figure 16, for the FCAW technique, an increase in the welding current results in increased weld bead height, depth of penetration, and weld bead width. These observations may be attributed to the increase in the welding current, which increases the melting rate of the filler wire. This, in turn, leads to more molten metal being deposited, contributing to an increase in bead height [39]. A higher welding current also results in an increase in the droplet temperature, causing smaller droplets to form more frequently. Additionally, the increased temperature enhances the falling velocity of the droplets, and their momentum influences the penetration depth. Consequently, higher welding currents contribute to achieving a deeper weld bead. Moreover, the elevated current increases the heat input, enlarging the melting volume of the workpiece and subsequently increasing the bead width [40].

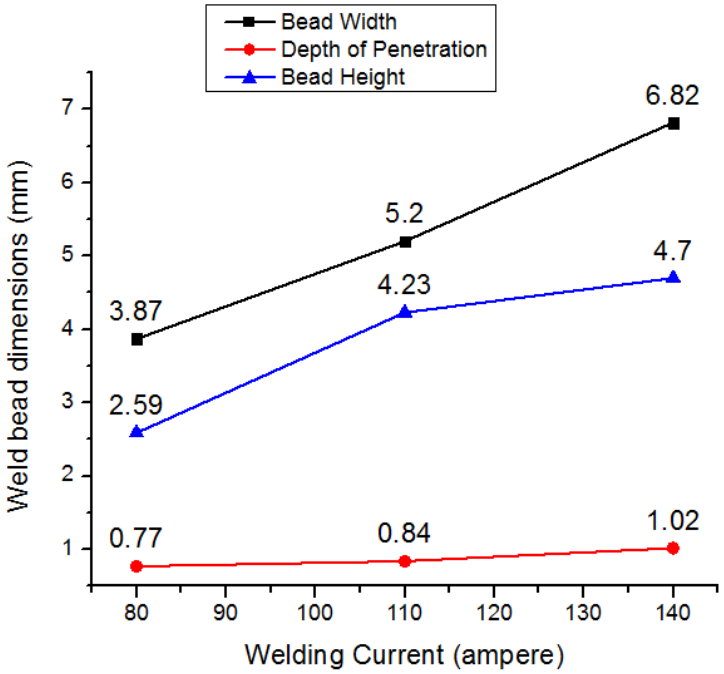

Figure 15 Effect of the welding current on the BW, DOP, and BH in the RMD technique

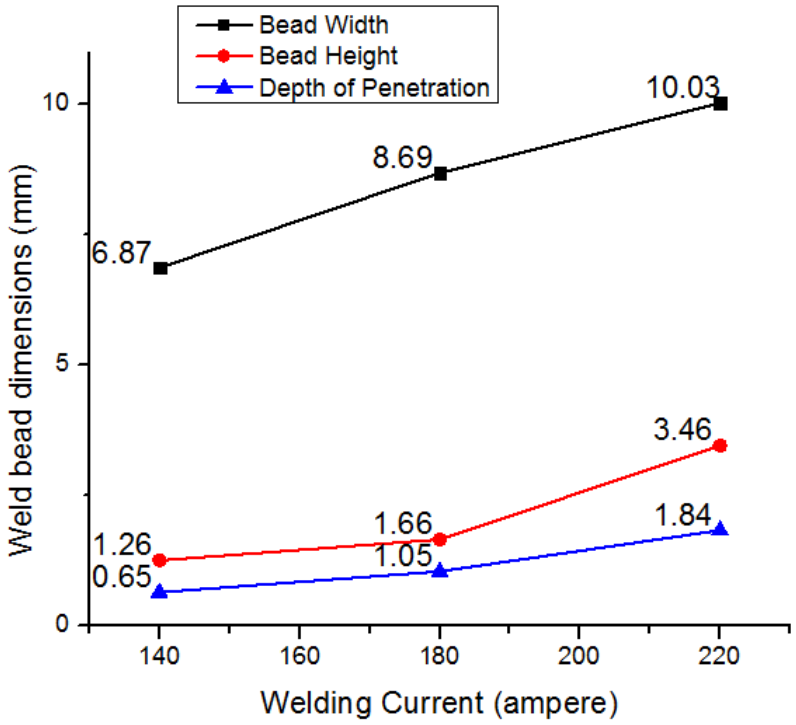

Figure 16 Effect of the welding current on the BW, DOP, and BH in the FCAW technique

3.5. Effect of voltage:

The influence of voltage on bead width, depth of penetration, and bead height at a current of 110 amperes in the RMD welding technique is shown in Figure 17. In contrast, Figure 18 illustrates the effect of voltage on these parameters at a current of 180 amperes in the FCAW welding technique. Figure 17, which illustrates the RMD technique, clearly shows that increasing the voltage leads to an expansion in bead width, accompanied by a reduction in both bead height and depth of penetration. Similarly, as shown in Figure 18, for the FCAW technique, an increase in voltage leads to an increase in bead width, whereas the bead height and depth of penetration decrease. These effects may be attributed to the fact that an increase in the arc voltage results in higher heat input during welding. The bottom diameter of the arc expands with increasing arc voltage, leading to increased heating and melting at the workpiece surface [41, 42]. Consequently, a wider weld bead is obtained at a higher arc voltage. Notably, the increased arc voltage does not affect the droplet formation frequency, droplet temperature, droplet falling velocity, or momentum of the droplets [40]. As a result, the penetration depth of the weld does not increase with increasing voltage. The decrease in weld bead height can be attributed to the simultaneous increase in bead width and the reduction in the electrode deposit area with increasing arc voltage [42].

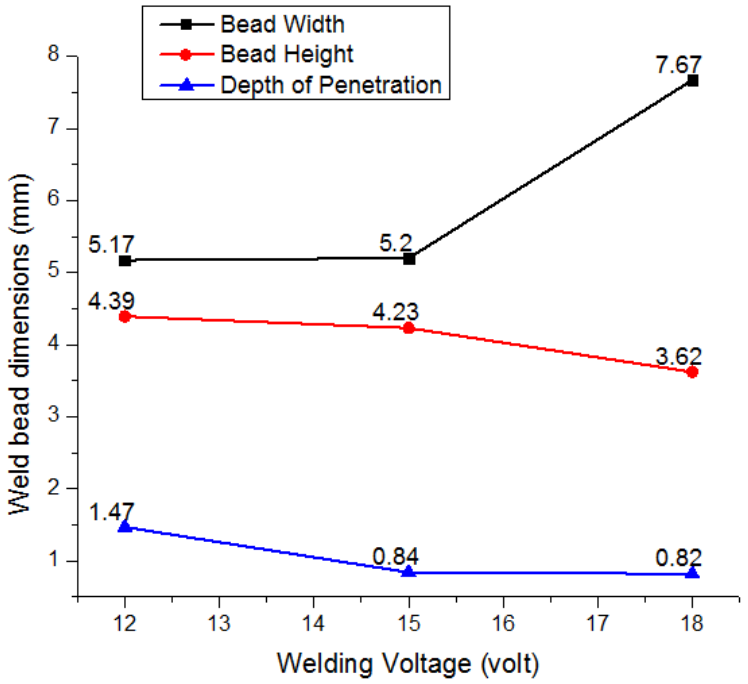

Figure 17 Effect of voltage on BW, DOP, and BH in the RMD technique

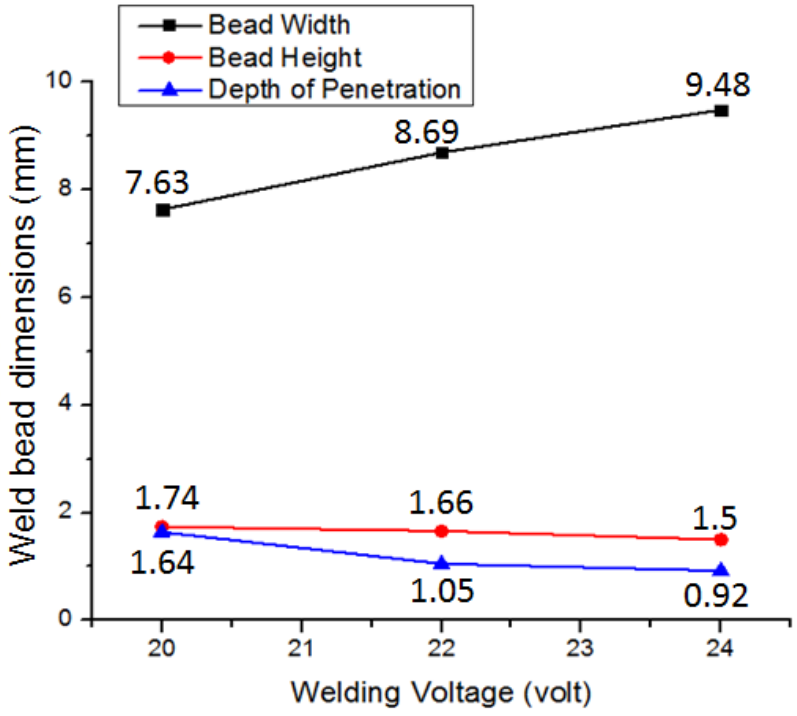

Figure 18 Effect of voltage on the BW, DOP, and BH in the FCAW technique

3.6. Effect of heat input:

As depicted in Tables 7 and 8, the bead-on-plate trials for the RMD technique, specifically trials E and G, and the bead-on-plate trials for the FCAW process, namely, trials 1 and 2, exhibit nearly identical heat inputs of approximately 0.36 KJ/mm. Upon comparing the weld bead geometries of these RMD and FCAW bead-on-plate trials, the data from Tables 5 and 6 reveal that, under these specified conditions, the FCAW technique results in a greater weld bead width than the RMD technique does. This difference can be attributed to the higher voltage utilized in the FCAW process than in the RMD technique, as the elevated voltage in the FCAW tends to broaden the weld bead [40]. Conversely, the bead height is more pronounced in the RMD technique than in the FCAW technique. This disparity arises from the use of a solid wire in the RMD technique, which facilitates a higher deposition rate than the flux-cored wire does [43]. Additionally, the root run deposited by the RMD technique exhibited a flat profile with no apparent convexity or concavity, and it was thicker than traditional GMAW root [16]. Moreover, the FCAW process yields a shallower depth of penetration than the RMD technique does. This observation may be attributed to the influence of the arc voltage on the arc length, where a decrease in the arc length leads to a narrower arc cone and a more focused arc. This phenomenon results in greater depth of penetration in the RMD technique [32].

Table 7 – Heat input for RMD process

Experiment	Current (A)	Voltage (V)	Travel Speed (mm/min)	Heat input (KJ/mm)
A	80	12	255	0.23
B	80	15	261	0.28
C	80	18	267	0.32
D	110	12	279	0.28
E	110	15	286	0.35
F	110	18	300	0.40
G	140	12	281	0.36
H	140	15	279	0.45
I	140	18	364	0.42

Table 8 – Heat input for RMD process

Experiment	Current (A)	Voltage (V)	Travel Speed (mm/min)	Heat input (KJ/mm)
1	140	20	486	0.35
2	140	22	503	0.37
3	140	24	414	0.49
4	180	20	400	0.54
5	180	22	387	0.61
6	180	24	387	0.67
7	220	20	375	0.70
8	220	22	343	0.85
9	220	24	324	0.98

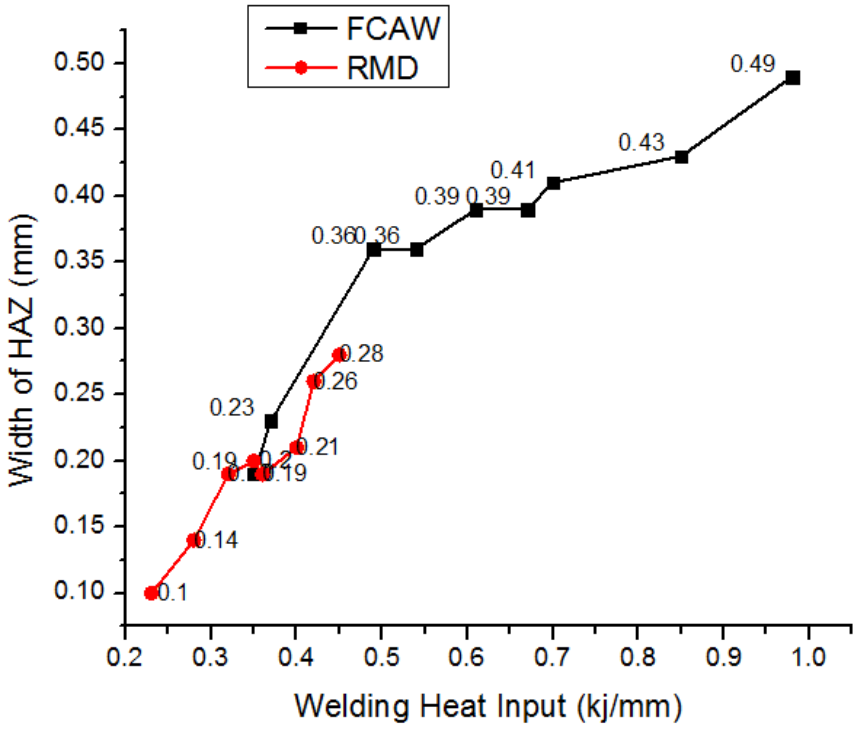

Figure 19 Effect of the welding heat input on the width of the HAZ for the RMD and FCAW techniques

Figure 19 illustrates the influence of the welding heat input on the width of the heat-affected zone (HAZ) for both the RMD and FCAW techniques. As depicted in Figure 20, there is a positive correlation between the increase in heat input and the widening of HAZ. This relationship may be anticipated because as the heat input increases, more energy becomes available to impact the microstructure of the material adjacent to the weld, resulting in a broader HAZ. [44]. Figure 21 also presents a comparison of heat input between the RMD and FCAW welding techniques, revealing that the FCAW process results in higher heat input than does the RMD technique. Among all eighteen experiments involving RMD and FCAW bead–on–plate trials, four exhibit nearly identical heat input levels. Specifically, experiment E and experiment 1 both demonstrate similar heat input of 0.35 kJ/mm, whereas experiment G and experiment 2 almost match the heat input values of 0.36 kJ/mm and 0.37 kJ/mm, respectively. Comparing these trials, which share the same heat input, in terms of bead width, bead height, depth of penetration, and width of the HAZ, yields intriguing insights.

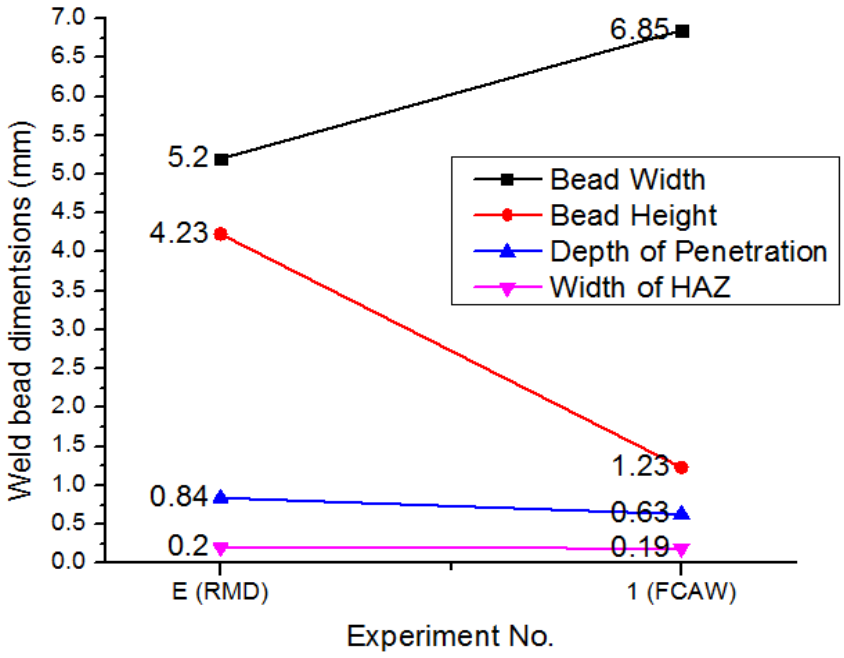

Figure 20 Comparison of weld bead dimensions between Experiment E and Experiment 1

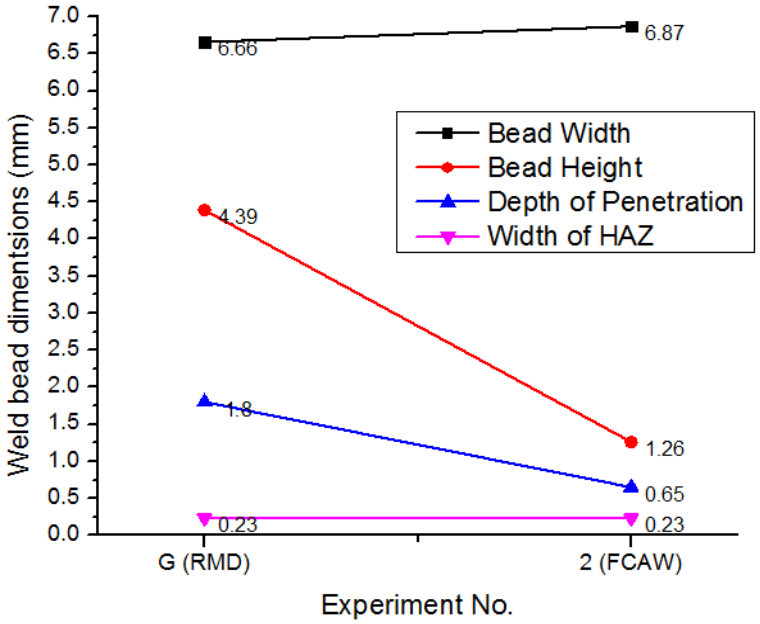

Figure 21 Comparison of weld bead dimensions between Experiments G and 2

Figure 21 shows a comparison of the weld bead dimensions between experiment E and experiment 1. At the same heat input of 0.35 kJ/mm, the width of the heat-affected zone is similar, and the depth of penetration is greater in experiment E than in experiment 1. However, the bead width is greater in experiment 1, which was deposited by the FCAW process, than in experiment E, which was deposited by the RMD process. Conversely, the bead height is greater in experiment E, which was deposited by the RMD process, than in experiment 1, which was deposited by the FCAW process. Similarly, Figure 22

represents the comparison of weld bead dimensions between experiment G and experiment 2, which almost match heat input values of 0.36 kJ/mm and 0.37 kJ/mm, respectively. The same trends observed in Figure 20 are evident in Figure 21. In the FCAW process, the wider bead width is due to the flux-cored wire's higher deposition rate than that of the solid wire. Moreover, FCAW's operation at higher voltage settings broadens the arc, leading to increased bead width compared with RMD [45–47]. Conversely, the RMD operates at lower voltage settings, contributing to narrower and taller bead heights. RMD technology allows precise control over metal transfer and deposition rates, maintaining higher bead heights while fine tuning the arc to deposit more metal onto the workpiece without compromising bead quality. While the higher voltage in FCAW broadens the arc and increases the bead width, it may result in slightly shallower penetration than RMD does [16, 48, 49].

4. Conclusions:

The present work uses RMD and FCAW welding procedures to investigate welded 316LN samples via bead-on-plate techniques. It evaluates the impact of current, voltage, and heat input on weld parameters such as bead height, width, penetration depth, and heat affected zone (HAZ) width. Visual inspection reveals various characteristics: at 80 A in RMD, the welded beads are uneven and narrow, whereas at 220 A in FCAW, spatter occurs. Undercuts result from higher currents in the RMD. Despite achieving full penetration, the RMD method results in a greater bead height and penetration depth but narrower bead and HAZ widths than the FCAW method does, which results in wider beads and HAZ but lower bead height and penetration. In both procedures, the bead height, width, and penetration are improved by increasing the welding current. An increased voltage in the RMD lengthens the bead but shortens its height and penetration, similar to the FCAW. The heat input increases the HAZ width, with the FCAW showing a wider HAZ due to its higher heat. At equivalent heat inputs, the RMD results in greater penetration and bead height, whereas the FCAW results in a wider bead width.

References

1. Kumar DH, Reddy a. S (2013) Study of Mechanical Behavior in Austenitic Stainless Steel 316 Ln Welded Joints. Int J Mech Eng Robot Res 2:1–22

2. Vasantharaja P, Vasudevan M, Maduraimuthu V (2018) Effect of Arc Welding Processes on the Weld Attributes of Type 316LN Stainless Steel Weld joint. Trans Indian Inst Met 71:127–137. https://doi.org/10.1007/s12666-017-1162-2

3. Fan Y, Wang K, Wang XY, et al (2021) Microstructures and mechanical properties of the fusion zone of 316L-316LN stainless steel multi-pass gas tungsten arc welded joint. J Mater Sci 56:17306–17318. https://doi.org/10.1007/s10853-021-06387-y

4. Patel NP, Badheka VJ, Vora JJ, Upadhyay GH (2019) Effect of Oxide Fluxes in Activated TIG Welding of Stainless Steel 316LN to Low Activation Ferritic / Martensitic Steel (LAFM) Dissimilar Combination. Trans Indian Inst Met. https://doi.org/10.1007/s12666-019-01752-7

5. Sireesha M, Albert SK, Shankar V, Sundaresan S (2000) Comparative evaluation of welding consumables for dissimilar welds between 316LN austenitic stainless steel and Alloy 800. J Nucl Mater 279:65–76. https://doi.org/10.1016/S0022-3115(99)00275-5

6. Awale DD, Ballal AR, Thawre MM (2020) Dissimilar weld joints of P91 and 316LN for power plants Applications-A review. Mater Today Proc 28:2505–2510. https://doi.org/10.1016/j.matpr.2020.05.003

7. Wenkai X, Li Z, Fuju Z, et al (2015) Effect of heat input on cryogenic toughness of 316LN austenitic stainless steel NG-MAG welding joints with large thickness. Mater Des 86:160–167. https://doi.org/10.1016/j.matdes.2015.07.115

8. Vasudevan M (2017) Effect of A-TIG Welding Process on the Weld Attributes of Type 304LN and 316LN Stainless Steels. J Mater Eng Perform 26:1325–1336. https://doi.org/10.1007/s11665-017-2517-x

9. Mohandas T, Reddy GM, Naveed M (1999) A comparative evaluation of gas tungsten and shielded metal arc welds of a `` ferritic ' ' stainless steel. 94:133–140

10. Singaravelu DL, Rajamurugan G, Devakumaran K (2018) Modified Short Arc Gas Metal Arc Welding Process for Root Pass Welding Applications. Mater Today Proc 5:7828–7835. https://doi.org/10.1016/j.matpr.2017.11.463

11. Das S, Vora JJ, Patel V, et al (2021) Experimental investigation on welding of 2.25 Cr-1.0 Mo steel with regulated metal deposition and GMAW technique incorporating metal-cored wires. J Mater Res Technol 15:1007–1016. https://doi.org/10.1016/j.jmrt.2021.08.081

12. Cuhel J (2008) Modified GMAW for Root Passes. TPJ - Tube Pipe Journal® - Fabr 1–4

13. Roth M (2009) Shinn Mechanical Uses PipeWorx Welding System to Increase Pipe Fabrication Quality and Productivity. Mill Electr Mfg LLC 1–4

14. Depo M, Depo M, Rmd T, et al (2020) Wel d ing Soft w a r e ove r come s s ho r t ci r c u it M I G limitation s . g ab d. 1–4

15. Ryan J (2018) Mechanical Contractor Diversifies and Redefines Business to Meet the Demand of the Mid-Atlantic Steel , Oil and Gas Industries. Mill Electr Mfg LLC 1–4

16. Das S, Vora JJ, Patel V (2019) Regulated Metal Deposition (RMD™) Technique for Welding Applications: An Advanced Gas Metal Arc Welding Process. Adv Weld Technol Process Dev 23–32. https://doi.org/10.1201/9781351234825-2

17. Demenin MF (2023) Root Welding Using the Regulated Metal Deposition Technology (Review). Power Technol Eng 57:123–128. https://doi.org/10.1007/s10749-023-01632-7

18. J. B (1956) Byrne J. Mechanical contractor increases pipe welding productivity up to 500 %. 2018. p. 1–8. 1–8

19. Roth M (2009) Graham Corporation Meets Reduced Rework Objectives With Help from Miller's PipeWorx™ Welding Systems. Mill Electr Mfg LLC 1–4

20. Bandhu D, Goud EV, Vora JJ, et al (2023) Influence of Regulated Metal Deposition and Gas Metal Arc Welding on ASTM A387-11–2 Steel Plates: As-deposited Inspection, Microstructure, and Mechanical Properties. J Mater Eng Perform 32:1025–1038. https://doi.org/10.1007/s11665-022-07185-6

21. Bandhu D, Djavanroodi F, Shaikshavali G, et al (2022) Effect of Metal-Cored Filler Wire on Surface Morphology and Micro-Hardness of Regulated Metal Deposition Welded ASTM A387-Gr.11-Cl.2 Steel Plates. Materials (Basel) 15:. https://doi.org/10.3390/ma15196661

22. Katherasan D, Sathiya P, Raja A (2013) Shielding gas effects on flux cored arc welding of AISI 316L (N) austenitic stainless steel joints. Mater Des 45:43–51. https://doi.org/10.1016/j.matdes.2012.09.012

23. Lathabai, S., & Stout RD (1985) "Shielding gas and heat input effects on flux cored weld metal properties." Weld journal, 64(11), 303s-313s 64:303–313

24. De Paz, Ronaldo R., Gabriel P. Famadico, Allysa Mariel J. Ortiz, Raymund Carlo F. Tanap, Reylina Garcia Tayactac, Edward B. Ang, Ricky D. Umali and JH (2023) Analysis on the industrial applications of flux cored arc welding on an international scale. 4th Int Conf Mech Intell Manuf Technol (ICMIMT), pp 135-142 IEEE, 2023

25. Amit Kumar, Vijayakumar P (2023) Comparison of Weld Built-up by FCAW and MIG Welding on Damaged Low Cr-Mo Alloy Steel Tube in Boiler Application. Int J Sci Res Arch 8:492–505. https://doi.org/10.30574/ijsra.2023.8.2.0243

26. Parvez M, Kumari P (2017) EFFECT OF MIG WELDING INPUT PROCESS PARAMETERS ON WELD

27. Kim IS, Kwon WH, Park CE (1996) The effects of welding process parameters on weld bead width in GMAW processes. J. KWS 14:204–213

28. Palani PK, Murugan N (2007) Optimization of weld bead geometry for stainless steel claddings deposited by FCAW. 190:291–299. https://doi.org/10.1016/j.jmatprotec.2007.02.035

29. Kurtulmus M, Bilici MK, Catalgol Z (2015) EFFECTS OF WELDING CURRENT AND ARC VOLTAGE ON FCAW WELD BEAD GEOMETRY. 23–28

30. Kumar D, Manidipto A (2015) Development of a Direct Correlation of Bead Geometry , Grain Size and HAZ Width with the GMAW Process Parameters on Bead-on-plate Welds of Mild Steel. https://doi.org/10.1007/s12666-015-0518-8

31. Das S, Vora J, Patel V, Bogum S (2021) Experience with advanced welding techniques (RMD & P-GMAW) with seamless metal cored wire for Oil & Gas pipeline industries. J Phys Conf Ser 1950:. https://doi.org/10.1088/1742-6596/1950/1/012043

32. Prajapati V, Dinbandhu, Vora JJ, et al (2020) Study of parametric influence and welding performance optimization during regulated metal deposition (RMD™) using grey integrated with fuzzy taguchi approach. J Manuf Process 54:286–300. https://doi.org/10.1016/j.jmapro.2020.03.017

33. Bandhu D, Abhishek K (2021) Assessment of weld bead geometry in modified shortcircuiting gas metal arc welding process for low alloy steel. Mater Manuf Process 36:1384–1402. https://doi.org/10.1080/10426914.2021.1906897

34. Welding AMMIG, Parameters C MIG Welding : Setting the Correct Parameters. 1–6

35. Conrardy C (2018) Guidelines For Gas Metal Arc Welding. Mill Electr Mfg LLC 1–17

36. Anon (1980) Structural Welding Code - Steel. Am Natl Stand Institute, Stand

37. Quintino L, Liskevich O, Vilarinho L, Scotti A (2013) Heat input in full penetration welds in gas metal arc welding (GMAW). https://doi.org/10.1007/s00170-013-4862-8

38. Cortéz VHL, Medina GYP, Valdéz FAR, López HF (2010) Effects of the Heat Input in the Mechanical Integrity of the Welding Joints Welded by GMAW and LBW Process in Transformation Induced Plasticity Steel (TRIP) Used in the Automotive Industry . 15:234–241

39. Kannan T, Murugan N (2006) Effect of flux cored arc welding process parameters on duplex stainless steel clad quality. 176:230–239. https://doi.org/10.1016/j.jmatprotec.2006.03.157

40. Lancaster, J.F. 1993. The Physics of Welding 2nd, Edition, Pergamon Press NY (1993) The Physics of Welding

41. Singh K, Pandey S (2009) Resources , Conservation and Recycling. 53:552–558. https://doi.org/10.1016/j.resconrec.2009.04.006

42. Murugan N, Gunaraj V (2005) Prediction and control of weld bead geometry and shape relationships in submerged arc welding of pipes. 168:478–487. https://doi.org/10.1016/j.jmatprotec.2005.03.001

43. Prajapati P, Badheka VJ, Mehta K (2018) An outlook on comparison of hybrid welds of different root pass and filler pass of FCAW and GMAW with classical welds of similar root pass and filler pass. Sadhana - Acad Proc Eng Sci 43:. https://doi.org/10.1007/s12046-018-0869-z

44. Kou S (2002) Welding Metallurgy. John Wiley & Sons, Inc.

45. Kamble AG, Rao RV (2013) Experimental investigation on the effects of process parameters of GMAW and transient thermal analysis of AISI321 steel. Adv Manuf 1:362–377. https://doi.org/10.1007/s40436-013-0041-2

46. Negash WT, Janaki RP (2023) Gas Metal Arc Welding Input Parameters Impacts on Weld Quality Characteristics of Steel Materials a Comprehensive Exploration Gas Metal Arc Welding Input Parameters Impacts on Weld Quality Characteristics of Steel Materials a Comprehensive Exploration. Manuf Technol 23:. https://doi.org/10.21062/mft.2023.046

47. Badheka VJ (2013) Effect of metal-cored arc welding process parameters on weld bead geometry. Weld Cut 2 106-111

48. Thakar HH, Chaudhari MD, Vora JJ, et al (2023) Performance optimization and investigation of metal-cored fi ller wires for high-strength steel during gas metal arc welding

49. Dinbandhu, Prajapati V, Vora JJ, et al (2020) Experimental studies of Regulated Metal Deposition (RMD™) on ASTM A387 (11) steel: study of parametric influence and welding performance optimization. J Brazilian Soc Mech Sci Eng 42:. https://doi.org/10.1007/s40430-019-2155-3